A molecular-dynamics study of the anisotropic surface-melting properties of Al(110)

D.J. Shu [a], D.Y. Sun [a], X.G. Gong [a,b,*], W.M. Lau [b]

[a] *Institute of Solid State Physics, Chinese Academia Sinica, 230031-Hefei, People's Republic of China*
[b] *Department of Physics and the Materials Science & Technology Research Centre, The Chinese University of Hong Kong, Shatin, N.T., Hong Kong*

Abstract

Surface melting of Al(110) was studied by molecular dynamics simulations with a well tested glue potential. We found that the surface began to disorder above 600 K via the formation of adatoms and vacancies. While bulk melting was observed at 945 K (experimental melting point is 933.5 K), the top four atomic layers were found to become liquid-like just before the bulk melts. Both the diffusion constants and the structure factors confirmed that surface melting of Al(110) was anisotropic, with random atom motion faster in the [1$\bar{1}$0] direction than in the [100] direction. On the other hand, in agreement with recent experimental observations [M. Polčik et al., Phys. Rev. Lett. 78 (1997) 491], our calculations showed the presence of a residual order preferentially along the [1$\bar{1}$0] direction via the presence of intact [1$\bar{1}$0] atom chain segments, even above 900 K. © 1999 Elsevier Science B.V. All rights reserved.

Keywords: Aluminum; Molecular dynamics; Surface melting

1. Introduction

In our conventional description of a crystal, its phase transformation from solid to liquid is relatively well-defined. At thermal equilibrium, the long-range order of the crystal is lost at its melting point. This concept applies to all atoms except those on the surface. In general, due to the additional surface free energy, the top surface layers may melt below the bulk melting point. The concept of surface melting was first suggested by Stranski in 1941 [1]. With the maturity of surface science techniques, the surface melting of Pb(110) was first verified experimentally by Frenken and van der Veen in 1985 [2]. Since then, surface melting has been studied extensively by means of experiments [3–9], theoretical modeling [10,11] and computer simulations [12–16].

The above surface energy consideration implies that close-packed surfaces should have a lower tendency to exhibit surface melting than more open surfaces for the same metal crystal [3]. Indeed, surface melting is evident on Pb(110), Al(110) and Cu(110) but does not occur on Pb(111), Al(111) and Cu(111) [6,12,15]. For those showing surface melting, the top layers losing long-range order are best described as quasi-liquid because they possess properties that are intermediate between those of a solid and the bulk liquid. As expected, both the thickness of this quasi-liquid region and the liquid-likeness in the region increase rapidly towards the bulk melting point.

Somewhat less expectedly, surface melting of

* Corresponding author. Fax: +86-551-5591434.
E-mail address: gong@theory.issp.ac.cn (X.G. Gong)

Pb(110) was found to be anisotropic by a low-energy electron diffraction experiment, with the [1$\bar{1}$0] rows losing long-range order more readily than the [001] rows [4]. In fact, the validity of the experimental evidence was questioned by a theoretical study [13], and was only recently confirmed independently by helium scattering experiments [5] and medium-energy ion-scattering experiments [7]. Even more interestingly, a more recent experimental study of the surface melting of Al(110) showed that the above description of anisotropy in surface melting should perhaps be modified, because intact atom chains were found preferentially in the [1$\bar{1}$0] direction in the quasi-liquid layer during surface melting of Al(110) [9].

Soon after the experimental report on surface melting, Stoltze et al. led the applications of molecular-dynamics techniques in the analysis of this intriguing surface behavior [12–14]. Although their work and other subsequent simulations by other research groups [15,16] on surface melting have indeed elegantly explained many experimental data in this topic, outstanding issues and new experimental data continue to urge for more theoretical simulations.

In this paper, we report on our molecular-dynamic simulations of the anisotropic melting of Al(110) which, to our knowledge, is the first attempt to study theoretically the formation and behavior of anisotropically oriented atom chains in the quasi-liquid layer of this interesting surface system. The rest of the paper is organized such that the details of the simulation methodology can be found in Section 2, results and discussion in Section 3, and conclusions in Section 4.

2. Simulation methodology

In this study, we used a numerical *glue* potential [17] to describe the atomic interactions, in which the potential energy is the sum of a pairwise term and a glue term:

$$V = \frac{1}{2} \sum_{ij} \Phi(r_{ij}) + \sum_i U\left(\sum_j \rho(r_{ij}) \right), \tag{1}$$

where $r_{ij} = |\mathbf{r}_i - \mathbf{r}_j|$ is the distance between the ith

and jth atom, $\Phi(r)$ is a short-range pair potential, and U is a many-body glue term. The parameters given by Ercolessi and Adams [17] were fitted with a large data base that included the ab initio atomic forces of many atomic configurations. With simulation of the condition for liquid–solid coexistence under equilibrium, the melting point of aluminum was determined to be 939 ± 5 K, close to the actual experimental datum of 933 ± 5 K. Further extensive tests have been performed to confirm that calculations using the glue potential can give other thermal and melting properties of aluminum solid and surfaces close to the corresponding experimental data [17].

Our simulation set-up for the study of Al(110) surface melting consisted of a slab of 20 atomic layers. Each atomic layer contained 16 atoms in the [1$\bar{1}$0] (y) direction and 10 atoms along the [001] (x) direction, 3200 atoms in total. Four layers at the bottom of the slab were fixed at the perfect face-centered cubic (fcc) positions to mimic the underlying infinite solid. The lattice parameters were adjusted according to the thermal expansion coefficient obtained from independent zero-pressure simulations [17]. Periodic boundary conditions were imposed in the lateral directions to mimic an infinite surface.

The simulations were carried out with the microcanonical ensemble approach. In all simulations the time step was set to 2.65 fs, with which Newton's equations of motion for atoms were integrated using the Verlet algorithm [18]. At each of the temperatures simulated, the equilibration took 265–600 ps. All physical properties were statistically averaged over the following 265 ps period.

To investigate the structural properties, first we defined the atomic number density distribution $\rho(z)$:

$$\rho(z) = \frac{1}{\sqrt{2\pi}\sigma} \sum_i e^{-(z - z_i)^2/2\sigma^2}, \tag{2}$$

where $z = 0$ is located at the fixed bottom of the slab and increases towards the free surface, z_i is the coordinate of the ith atom, the Gaussian expansion σ is set to 10% of the layer spacing along the [110] direction, and the sum is over all atoms.

The self-diffusion constant for the atoms in the topmost layer was obtained by:

$$D_s = \lim_{t \to \infty} \frac{R_s^2(t)}{2n_d t},$$ (3)

where n_d is the degree of dimension in calculating the mean-squared displacement (MSD), $R_s^2(t)$:

$$R_s^2(t) = \left\langle \frac{1}{N_s} \sum_{\alpha=1}^{n_d} \sum_{i \in s}^{N_s} [r_{i\alpha}(t+\tau) - r_{i\alpha}(\tau)]^2 \right\rangle,$$

$$r_\alpha = x, y, z.$$ (4)

In this equation, the angular brackets denote an averaging over the initial time τ, and N_s is the number of atoms in the topmost layer.

Furthermore, we used the squared layer structure factor $|S_l(K_\alpha)|^2$ as a parameter to measure the structural order of the lth atomic layer. $S_l(K_\alpha)$ was defined as:

$$S_l(K_\alpha) = \left\langle \frac{1}{n_l} \sum_{i \in l} e^{iK_\alpha \cdot r_i} \right\rangle, \quad \alpha = x, y,$$ (5)

where $K_y = (2\pi/a_0)(2, \bar{2}, 0)$ is along the atomic rows in the $[1\bar{1}0]$ direction, $K_x = (2\pi/a_0)(0, 0, 2)$ is across the rows, and the angular brackets indicate an averaging over the simulated trajectories.

3. Results and discussion

3.1. Surface melting

Since melting of a crystal is signified by the loss of its long-range order, this phase transition can be conveniently examined by monitoring the layer-by-layer modulation of the atom density profile of the crystal. In our study, the melting of Al(110) was examined by the density changes in the z direction as a function of temperature. The data are shown in Fig. 1, which demonstrates clearly that, at low temperatures, atoms in the bulk of the (110) crystal were packed in (110) planes with a constant density in each plane and virtually no atoms between these parallel layers. At 600 K the density of the first crystal layer was, however, slightly lower than that of the sub-surface layers. The loss was compensated by a small density
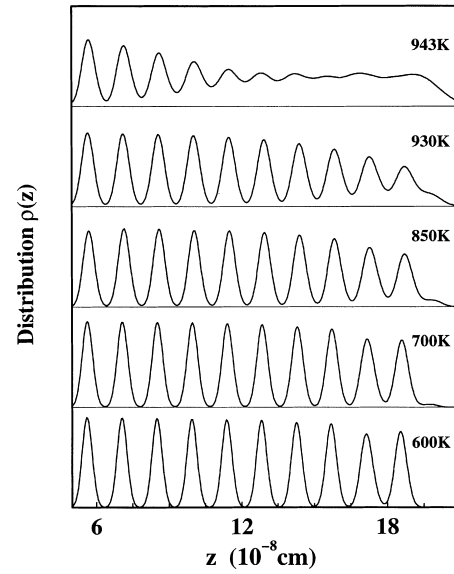

Fig. 1. Atomic density distribution $\rho(z)$ as a function of temperature, with z denoting the distance normal to the Al(110) surface.

above the crystal layer. Accordingly, some atoms of the first crystal layer left the layer and became adatoms. The generation of vacancies/adatoms induced disorder and converted the first crystal layer into a quasi-liquid.

An increase of temperature above 600 K further randomized the layer modulation of the density profile. At 943 K, the top four layers of the original crystal became liquid-like. At 945 K, the layer modulation of the entire crystal was lost. As such, the melting point of the crystal modeled was 945 K. By comparison, the experimental melting point of aluminum is 933.5 K. Regarding the formation of quasi-liquid, it was shown experimentally [6] that, just below the melting point, there are about five quasi-liquid layers on Al(110).

The data shown in Fig. 1 show that, unlike bulk melting which occurred at a very narrow temperature window, the phenomenon of surface melting was evident in a rather wide temperature span. To seek a more well-defined means to characterize surface melting, we examined the relationship between total energy per atom and temperature. Such a relationship is shown in Fig. 2. While the sharp change at 945 K denoted a phase transition
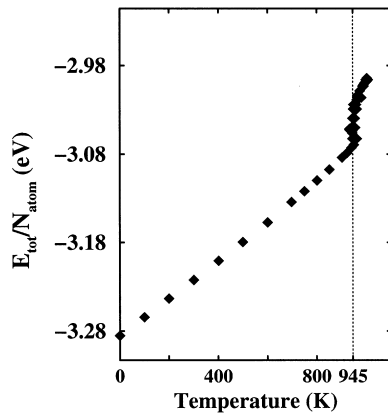
Fig. 2. Total energy per atom as a function of temperature. The vertical dotted line indicates the calculated melting point at 945 K.

Fig. 3. Diffusion constants as a function of $1/T$.

from solid to liquid, the soft deflection at around 700–750 K could be a convenient definition of the onset temperature of surface melting. An examination of the most recent experimental data on surface melting of Al(110) [9] also indicates an onset temperature in the range of 700–800 K.

3.2. Anisotropy in surface melting

In the framework of atom diffusion, we found (as shown in Fig. 1) that even at a relatively low temperature of 600 K, some atoms of the first crystal layer could diffuse off the layer to create vacancies and adatoms. When the diffusion constants for the first crystal layer along the [001] direction (defined as 'x'), the [1$\bar{1}$0] direction ('y') and the normal direction ('z') are compared, as summarized in Fig. 3, one can see clearly that diffusion along [1$\bar{1}$0] was faster than in the other two directions. As such, the layer was more liquid-like in the [1$\bar{1}$0] than the [001] direction, in terms of average atom motion. This anisotropy in surface melting of Al(110) is consistent with the anisotropic properties reported on Pb(110) [4,5,7].

By fitting the data below 940 K in Fig. 3, we obtained the activation energy U_D for surface diffusion; we found U_D to be 0.59 eV and 0.47 eV for the components along x and y, respectively. By comparison, the activation energy for diffusion involving atoms in the bulk is 1.28 eV as deter-
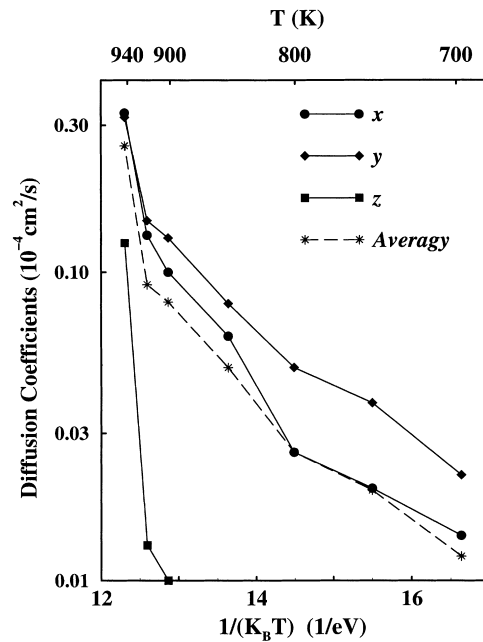
mined by experiments [19,20] and 1.30 eV as calculated by the glue potential model [17]. Once again, the surface region of Al(110) is 'softer' than its bulk, and average atom motion along the [1$\bar{1}$0] direction is more ready than that in the [100] direction. The directional difference in diffusion activation energy can be explained by the fact that atoms of the [1$\bar{1}$0] rows are closely packed, over which atoms or segments of atoms can glide relatively easily.

The directional difference in average atom motion can also be seen by analyzing the vibrational characteristics of the Al(110) surface. In this analysis, we calculated the mean-square amplitudes of vibration (MSAVs) along the directions x, y and z as a function of temperature. The data are shown in Fig. 4. The MSAVs calculated along these three directions increased linearly with temperature, like the behavior of a harmonic system, up to 600 K. Above 600 K, MSAVs in all directions increased sharply. The vibration amplitude along the y direction was once again much larger than that along the x direction, which is consistent with the anisotropy concluded in the analysis of atom diffusion.
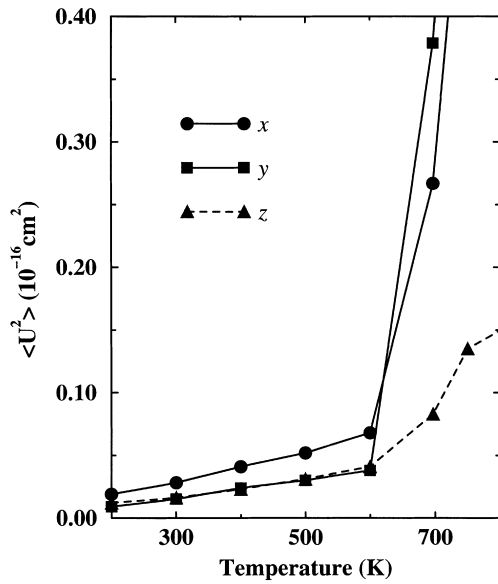
Fig. 4. Mean-square amplitudes of vibration (MSAVs) for surface atoms along three orthogonal directions (x, y, z).

the atoms were more diffusive in the y direction, $|S(K_y)|^2$ was smaller than $|S(K_x)|^2$. The anisotropy factors, defined as the difference between the squared layer structure factors in x and y $[|S(K_x)|^2 - |S(K_y)|^2]$, are also included in Fig. 5 to further clarify the structural differences in the [001] and [1$\bar{1}$0] directions.

3.3. Chain of atoms

In agreement with a recent experimental report [9] on surface melting of Al(110), our calculations showed the presence of atom chains along the [1$\bar{1}$0] direction in the process of surface melting. In our simulations, atoms were considered to form a chain if their pairwise interatomic distance was smaller than a certain cutoff value, R_{cut}. The chain length (N), defined as the average number of atoms per chain, is given in Fig. 6 as a function of temperature, in the format of log N versus $1/T$. Since there is no standard value for R_{cut}, we calculated the chain length using four different

In addition to the preceding data, the squared layer structure factors, $|S(K_x)|^2$ and $|S(K_y)|^2$, and their difference, are shown in Fig. 5 as a function of temperature for the topmost seven layers. Since
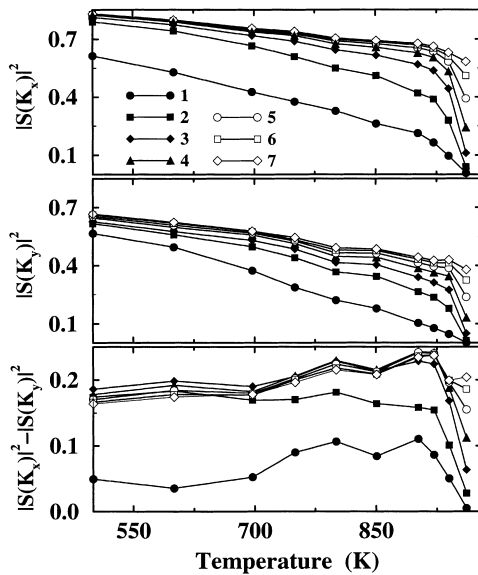

Fig. 5. Temperature dependence of the squared layer structure factors $|S(K_x)|^2$ and $|S(K_y)|^2$, and their difference, for the first seven layers.
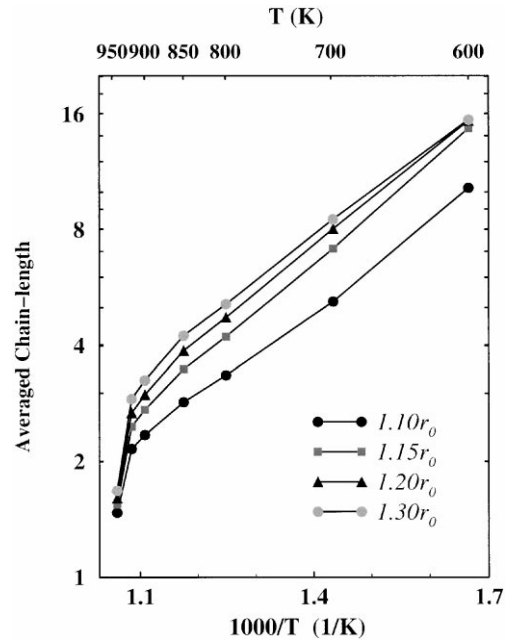

Fig. 6. Temperature dependence of the averaged length of atomic chains along the [1$\bar{1}$0] direction on Al(110) in the liquid-like top surface layer below the bulk melting point, for four different R_{cut} values.

values of R_{cut} in reference to the standard Al—Al bond length. For this data range, we found that all R_{cut} gave qualitatively the same results. In general, chain length decreased exponentially with a reduction in reciprocal temperature.

We fitted the 'chain length versus temperature' data in the window of 600 to 850 K with $\exp(\alpha/kT)$, where k is the Boltzmann constant, and found an α value in the range of 0.22–0.27 eV for the four different R_{cut} values. It is interesting to note that the value of α is close to the formation energy of a vacancy for the first layer (~ 0.3 eV) [12]. In fact, if we consider the chain segment formation as a result of breaking a long atom row into a number of chain segments, the number of segments per unit length is equal to the reciprocal of the chain length ($1/N$). As such, the attribute $1/N$ reflects the chain segment formation probability. In the relationship of $1/N$ versus $\exp(\alpha/kT)$, α thus represents the activation energy for changing a long atom row into chain segments. Indeed, conceptually, the formation of vacancy in a long atom row is equivalent to partitioning the atom row into chain segments.

The plot in Fig. 6 shows that, in the temperature range of 850–950 K, the temperature dependence of chain length was different from that in the range of 600–850 K. The difference suggests that the chain formation mechanism in the high-temperature regime was no longer determined simply by vacancy formation. If we follow the preceding concept of activation energy for changing a long atom row into chain segments, the chain formation mechanism in the temperature range of 900–950 K was dominated by a process with an activation energy significantly higher than 0.25 eV.

As mentioned earlier, the presence of residual order on Al(110) during surface melting preferentially along the [1$\bar{1}$0] direction was first demonstrated experimentally with the evidence of atom chains in the [1$\bar{1}$0] direction [9]. The chain length at 900 K was determined to be at or above four. In the present study, the average chain length at 900 K was estimated to be about three. Hence, the two sets of data are quite close. We agree with the interpretation given by Polčik et al. [9] that the presence of the intact [1$\bar{1}$0] chains is due to energy minimization at a solid–liquid interface

[15,16]. In our own extension of such an interpretation, we treat a liquid as a randomly close-packed phase. As such, the aluminum quasi-liquid layer will tend to assume a (111) close-packed form. However, the minimization of interfacial energy further requires the matching of the quasi-liquid structure with that of the solid substrate, which assumes a (110) surface structure. Accordingly, the alignment of some of the close-packed atom rows in the quasi-liquid layer with the atom row in the [1$\bar{1}$0] direction of the solid substrate will be particularly favorable in energy. Atoms not belonging to the aligned rows in the quasi-liquid are not supported by the solid substrate structure, and will thus depart randomly. The partial order in the quasi-liquid layer along the [1$\bar{1}$0] direction of the solid is thus established.

4. Summary

By using molecular-dynamics simulations with the glue potential, we have studied the Al(110) surface in the temperature range from 200 K to its melting point. In this temperature range, we have investigated properties such as the atom number density $\rho(z)$, mean-squared vibrational amplitudes, diffusion constants, static structure factors and averaged length of atom chains in the liquid-like layer along the [1$\bar{1}$0] direction of the solid substrate. We found that, in agreement with experiments, the Al(110) surface began to disorder at 600 K by the generation of adatoms and vacancies. The disorder spread from the top layer to deeper layers as the temperature increased, and the first four crystal layers became quasi-liquid just before bulk melting took place. However, surface melting was anisotropic, with higher average atom motion along the [1$\bar{1}$0] direction than that along the [100] direction due to the close-packed nature of the atom rows of the solid phase in the [1$\bar{1}$0] direction. Ironically, such a nature and the minimization of interface energy gave rise to the persistence of partial order of the liquid-like layer in the [1$\bar{1}$0] direction of the solid phase by aligning close-packed atoms in the liquid-like layer with those of the atom rows of the solid phase in the [1$\bar{1}$0] direction.

Acknowledgements

References

[1] I.N. Stranski, Naturwissenschaften 29 (1941) 743.

[2] J.W.M. Frenken, J.F. Van der Veen, Phys. Rev. Lett. 54 (1985) 134.

[3] B. Pluis, A.W.D. van der Gon, J.W.M. Frenken, J.F. van der Veen, Phys. Rev. Lett. 59 (1987) 2678.

[4] K.C. Prince, U. Breuer, H.P. Bonzel, Phys. Rev. Lett. 60 (1988) 1146.

[5] J.W.M. Frenken, B.J. Hinch, J.P. Toennies, Ch. Wöll, Phys. Rev. B 41 (1990) 938.

[6] A.W.D. van der Gon, R.J. Smith, J.M. Gay, D.J. O'Connor, J.F. van der Veen, Surf. Sci. 227 (1990) 143.

[7] A.W.D. van der Gon, H.M. van Pinxteren, J.W.M. Frenken, J.F. van der Veen, Surf. Sci. 244 (1991) 259.

[8] W. Theis, K. Horn, Phys. Rev. B 51 (1995) 7157.

[9] M. Polčik, L. Wilde, J. Hasse, Phys. Rev. Lett. 78 (1997) 491.

[10] A. Trayanov, E. Tosatti, Phys. Rev. Lett. 59 (1987) 2207.

[11] O. Tomagnini, F. Ercolessi, S. Iarlori, F.D. Di Tolla, E. Tosatti, Phys. Rev. Lett. 76 (1996) 1118.

[12] P. Stoltze, J.K. Nørskov, U. Landman, Phys. Rev. Lett. 61 (1988) 440.

[13] P. Stoltze, J.K. Nørskov, U. Landman, Surf. Sci. 220 (1989) L693.

[14] P. Stoltze, J. Chem. Phys. 92 (1990) 6306.

[15] H. Häkkinen, M. Manninen, Phys. Rev. B 46 (1992) 1725.

[16] A. Landa, P. Wynblatt, H. Häkkinen, R.N. Barnett, U. Landman, Phys. Rev. B 51 (1995) 10972.

[17] F. Ercolessi, J.B. Adams, Europhys. Lett. 26 (1994) 583.

[18] M.P. Allen, D.J. Tildesley, in: Computer Simulation of Liquids, Oxford University Press, New York, 1987, p. 78.

[19] R. Stedman, G. Nilsson, Phys. Rev. 145 (1966) 492.

[20] M.J. Fluss, L.C. Smedskjaer, M.K. Chason, D.G. Legnini, R.W. Siegel, Phys. Rev. B 17 (1978) 3444.